Int J Mater Form (2018) 11:325–337
DOI 10.1007/s12289-017-1351-x

SI: MODELING MATERIALS AND PROCESSES, IN MEMORY OF PROFESSOR JOSÉ J. GRÁCIO

Numerical study of springback using the split-ring test: influence of the clearance between the die and the punch

V. M. Simões[1,2] · M. C. Oliveira[2] · D. M. Neto[2] · P. M. Cunha[2] · H. Laurent[1] · J. L. Alves[3] · L. F. Menezes[2]

Received: 31 December 2016 / Accepted: 23 March 2017 / Published online: 21 April 2017

Abstract The split-ring test consists in cutting a ring from the wall of a drawn cylindrical cup, which is split to measure the springback. This springback measure can also be used to estimate the circumferential residual stresses in the ring. It is known that the distribution of the residual stresses in the cup depends on the specific combination of forming parameters selected to perform the deep drawing operation, which include the depth of the cup and the clearance between the die and the punch. Moreover, the forming parameters also seem to affect the distribution of the axial and circumferential through-thickness stress profiles along the cup height, since different ring opening trends have been observed, when rings are cut from the cup wall at different heights. The focus of this numerical study is the analysis of the impact of an ironing stage on the residual stress distributions in the cylindrical cup and, consequently, in the split-ring test. The analysis is performed considering a 6016-T4 aluminium alloy, for which experimental results are available. The results show that the ironing of the vertical wall changes the characteristic distribution of the axial and circumferential residual stresses in all locations of the cup wall, even for relatively small ironing strains. This affects the trend observed for the ring opening value, when rings are cut at different heights.

Keywords Springback · Split-ring test · Finite element analysis · Ironing · Residual stresses

Introduction

The split-ring test was proposed as a springback benchmark test since it allows avoiding the problems related with the accurate measurement of springback. In fact, the use of a stamped component as the reference shape normally requires: (i) measurement fixtures that should not influence actual springback values by not restraining the formed part; and (ii) profiling equipment such as coordinate measuring machines or laser scanning, with a proper definition of the measurement

✉ M. C. Oliveira
marta.oliveira@dem.uc.pt

V. M. Simões
vasco.simoes@uc.pt

D. M. Neto
diogo.neto@dem.uc.pt

P. M. Cunha
patrick.cunha@uc.pt

H. Laurent
herve.laurent@univ-ubs.fr

J. L. Alves
jlalves@dem.uminho.pt

L. F. Menezes
luis.menezes@dem.uc.pt

[1] Univ. Bretagne Sud, FRE CNRS 3744, IRDL, F-56100 Lorient, France

[2] CEMMPRE, Department of Mechanical Engineering, University of Coimbra, Polo II, Rua Luís Reis Santos, Pinhal de Marrocos, 3030-788 Coimbra, Portugal

[3] CMEMS, Microelectromechanical Systems Research Unit, University of Minho, Campus de Azurém, 4800-058 Guimarães, Portugal

locations and directions. In many cases, most of the part will present a small springback which reduces the measurement accuracy, increasing the experimental error [1].

The split-ring test was proposed based on previous knowledge concerning the measurement of residual circumferential stresses at the surface of tubes or deep drawn cups. It consists on the cut of a ring specimen from the cup and its split longitudinally along any radial plane. The amount by which the outer diameter of the ring changes from its original value is a measure of the released residual circumferential stress. The distribution of the residual circumferential stress through the ring thickness must be determined or assumed, but it is possible to have good estimates of its magnitude based on the ring opening [1, 2].

A deep drawn cup presents significant residual stresses that result in large springback values when allowed to relax. The large springback increases indirectly the measurement accuracy and reduces the experimental error. Thus, the use of the ring opening as a standardized measure of springback enables the comparison of springback predictions using different numerical models, allowing the calibration of numerical and constitutive model parameters, to achieve a satisfactory correlation with the benchmark test results. In this context, it has been used to characterize the springback by many authors [1–8].

The accuracy of the springback prediction depends of the stress state achieved after forming, particularly its gradient through the sheet thickness. In this context, most of the studies on the analysis of residual stress, induced by forming processes and springback, resort to simpler plane strain geometries [9–12]. The springback that results from the split-ring test performed on a deep drawn cup is due to the stretch-bend process that occurs with the material flow. At the end of the forming, there are residual stresses in the cup because different locations accumulated different magnitudes of plastic strain. These stresses are a key factor for the springback, because their integral over the wall thickness yields a non-zero bending moment and thus a shape change when the ring is split [8]. The distribution of the residual stresses in the cup depends on the specific combination of forming parameters selected to perform the deep drawing operation, which include the depth and diameter of the cup, the bending radii of the tools, the gap between the die and the punch, the blank-holder force and the friction conditions. In this context, an increased depth of the cup can contribute to increase the homogeneous stretching, resulting in more uniform though-thickness circumferential and axial stresses distributions. The decrease of the bending radius of the die can cause excessive strains on both sides of the blank, reducing the springback at an increased risk of cracking on the outside, as a result of the higher tensile stresses installed [8]. However, this depends also on the combination of the other process parameters, because other authors showed that the die radius has a negligible influence on the circumferential stress distribution [2].

The stretch portion associated with the material flow depends of the restraining force applied by the blank-holder and the contact with friction conditions, meaning also that the residual stresses present in a cup are not the same for all points around and along the cup wall [1]. For the process conditions suggested in [1], it is expected that the residual stresses are largest near the top of the cup wall, due to the bending that occurred at the end of the draw, when little net tension was applied. This is confirmed by the results presented in [8] for an AISI-1010, which showed that the ring opening becomes larger for rings cut further away from the region in contact with the punch radius. However, in the analysis performed for a 6111-T4 aluminium alloy, the ring presenting the higher opening corresponds to one located closer to the middle of the vertical wall [3]. The tools dimensions used in both studies are the same, with a clearance between the die and the punch of 5 mm. However, the AISI-1010 sheet is 3.0 mm thick, while the 6111-T4 is only 0.925 mm. This indicates that the gap between the die and the punch can also affect the residual stresses distributions, as reported in [2], which show that for a clearance smaller than the blank thickness, the circumferential residual stress values are smaller. This can be related with the occurrence of an ironing stage, which has been previously reported to contribute to a reduction of the tensile residual stress values in the outer surface [13].

The residual stress distributions in the cup [13] and in the ring [7, 8] have been studied , highlighting their variation along the cup wall. In fact, in a study performed to evaluate the robustness of the split-ring test, it was found that the largest variation in the ring opening was observed when the location where the ring was cut from the sidewall was moved along the cup wall [4]. In that study, a decrease of the ring opening occurred when the ring was cut closer to the punch radius, which was associated to the corresponding decrease of the circumferential stresses toward the cup bottom. This was attributed to a rising level of accumulated plastic strain as the rings are closer to the bottom [7]. In fact, springback results from the amount of elastic energy stored in the part during the forming operation. Thus, by increasing the proportion of material submitted to plastic deformation, it is possible to reduce the change of shape induced by the elastic recovery.

The comparison of results obtained considering similar forming parameters, but different blank thicknesses (3.0 and 0.88 mm), indicates that the gap between the die and the punch results in a major discrepancy in the thickness distribution along the cup wall. For the thicker blank, the thickness value decreases toward the bottom, while for the thinner blank it increases slightly (but is still lower than the blank thickness). For the thick walled cup, a decrease in thickness is a clear indication of uniform vertical stretching (rising plastic strain), and it explains the lower springback at the cup bottom. This seems to be contradicted by the slight increase in thickness toward the bottom found for the thin walled cup. Although

there is no rise in the vertical stretching towards the cup bottom, the springback is still lower at the bottom. The explanation given by the authors is based on the different circumferential plastic flow of material during the deep drawing process, leading to higher levels of circumferential plastic strain for the thin walled cup, when compared with the thicker, where higher strains are predominantly caused by vertical stretching. Higher thickness differences along the vertical wall implies an increased circumferential material flow and higher strain levels. The latter have the effect of reducing springback as more material is deformed beyond the yield stress [4].

The results from previous studies indicate that the split-ring test is a robust springback benchmark [4], but improved knowledge is still required concerning the influence of the process parameters on the residual stresses distribution along the cup wall. In fact, experimental split-ring test results obtained in the analysis of a 6016-T4 aluminium alloy revealed a decreasing value for the ring opening with the increase of the distance from the cup bottom, which seemed to result from the fact that an ironing stage occurs during the cup forming. These results are discussed in the following section, where the forming process conditions are described, followed by the details about the numerical model adopted to perform the numerical study. The third section focus on the residual stresses distribution numerically predicted, as well as on the axial moment distribution along the cup wall, highlighting the impact of the clearance between the die and the punch and the forming depth. Finally, in the last section the main conclusions are discussed.

Description of the tests conditions

The forming process selected for the analysis and posterior springback evaluation using the split-ring test is the one used in [14], which was also proposed in the conference Numisheet 2016, as a benchmark to evaluate the springback of an AA5086 alloy under warm forming conditions [15]. The main dimensions of the tools (axisymmetric) are given in Table 1 and are schematically shown in Fig. 1. The gap between the die and the blank-holder is 1.125 mm. This means that when a 1 mm thick blank is used, if the blank thickens more than 0.125 mm, due to the compression stress state in the flange, an ironing stage will occur. The intensity of this ironing stage is strongly dependent on both the drawing ratio and the gap between the die and the punch. The circular blank presents a diameter of 60 mm, which results in a drawing ratio of 1.8.

Table 1 Main dimensions of the forming tools used in the deep drawing of a cylindrical cup [mm]

Die			Punch		Blank-holder
Opening diameter	Corner radius	Height	Diameter	Corner radius	Opening diameter
35.25	5.0	8.75	33.0	5.0	33.6

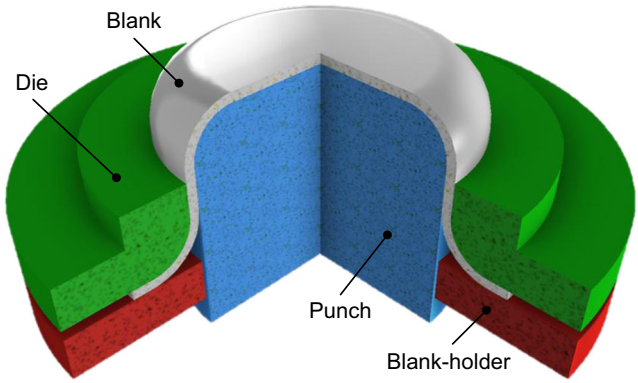

Fig. 1 Schematic representation of the forming tools considering a gap between the punch and the die of 1.125 mm

The material of the blank was taken from a rolled sheet of 6016-T4 aluminium alloy with 1.0 mm of thickness and uniaxial tensile tests were performed, enabling the identification of the material parameters required for the numerical analysis [16]. Moreover, the forming process previously described was performed using a blank-holder force of 6 kN. For further details concerning the forming tests experimental procedure, please refer to [16].

Two cups were fully drawn and three rings were trimmed at a distance of 7 mm from the cup's bottom with a height of 3 mm, with a distance between them of 2 mm, using an electro-erosion machine by wire. The positioning of the rings is schematically shown in Fig. 2 (a). The wire and the electric arc generate a cutting thickness of 0.3 mm, which is taken into account to obtain a ring of 3 mm in height. The same technique was used to split the rings along the RD. The average values obtained for the ring opening measurement from the two cups were 5.67, 4.23 and 2.12 mm, for the bottom, middle and top rings, respectively. This trend corresponds to a decreasing opening value along the cup's height. Therefore, it was decided to try to understand the impact of the ironing stage in the distribution of the residual stresses in the formed cups. This study was performed numerically, considering also two other drawing depth values of 16 and 22 mm, which are smaller than the standard value of 30 mm. For the smaller drawing depth values a single ring was cut from the cup wall, as exemplified in Fig. 2 (b), for the smaller punch displacement. Also, for the standard drawing depth, a different gap between the die and the punch was considered, using a value of 4 mm, obtained by reducing the punch diameter to 27.25 mm, which results in a drawing ratio of 2.2. This value for the clearance was selected taking as reference the one used in [3], and the tools dimensions used in the current study.

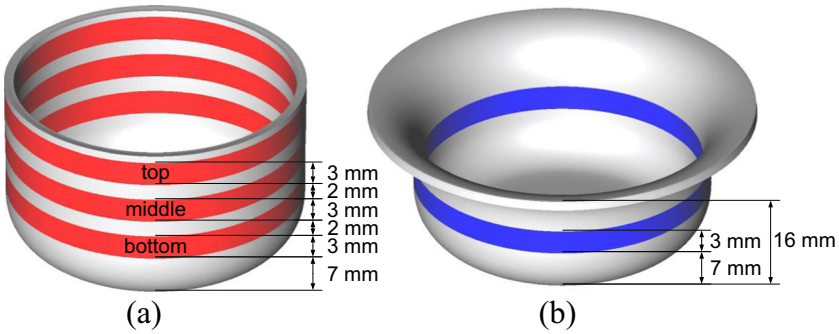

Fig. 2 Positioning of the ring(s) in the cylindrical cup: (**a**) fully drawn cup; (**b**) for a fixed punch displacement of 16 mm

Finite element model

In order to model the deep drawing process and the split-ring test, the finite element analysis is divided into four different stages: (i) deep drawing operation; (ii) unloading the cup; (iii) cutting the ring and (iv) split the ring. The numerical simulations were carried out with the in-house static implicit finite element code DD3IMP [17], specifically developed to simulate sheet metal forming processes [18–20]. The ring cut and splitting was performed with the in-house code DD3TRIM [21, 22].

Due to geometric and material symmetry conditions, only half model is simulated. This allows to simplify the analysis of the cutting and splitting stages, with the later performed by just removing the symmetry condition at one end of the ring. The blank is discretized with linear hexahedral finite elements, using a selective reduced integration technique [23] to avoid volumetric locking. The central zone of the blank (flat area of the punch) is discretized by a relatively coarse unstructured mesh, while the remaining zone is discretized with a fine in-plane structured mesh, corresponding to a total of 86 elements in the radial direction and 204 in the circumferential one. This discretization respects the recommendations of using an element size that covers 5 to 10° of the tool radius, i.e. at least 9 finite elements in contact with the radius of the die or punch, in order to accurately predict the springback [11, 12]. Springback prediction is known for being quite sensitive to the in-plane refinement but also to the number of integration points through-thickness and the integration rule adopted [12, 24]. In this study a total of 3 layers of elements through-thickness was considered, corresponding to 6 integration points in this direction, combined with the Gauss integration rule. The discretization of the blank comprises a total of 58,806 finite elements.

The forming tools are considered as rigid in the numerical simulation and its surfaces were discretized with Nagata patches [25]. The nodal normal vectors required for the smoothing method are evaluated from the IGES file, using the algorithm proposed in [26], which allows the recovery of the curvature of the surfaces with good accuracy [27] with a total of 369 Nagata patches. Further details about the blank and tools discretization can be found in [28].

Previous studies indicate that, for the conditions assumed in the experimental analysis, the deep drawing stage involves a drawing and an ironing operation. Besides, the springback prediction is quite sensitive to the numerical parameters but also to the constitutive model adopted. In this context, it was shown that the use of an orthotropic yield criterion generates a gradient for the stress distribution in the circumferential direction, which usually contributes to the underestimation of the springback [14, 29]. The 6016-T4 aluminium alloy under study presents a planar anisotropy coefficient of 0.038, which results in a small earing profile [16]. In this context, and in order to keep the results analysis as simple as possible, it was decided to assume an isotropic plastic behaviour of the material, described by the von Mises yield criterion:

$$\overline{\sigma}^{\,2} = (\sigma_{22}-\sigma_{33})^2 + (\sigma_{33}-\sigma_{11})^2 + (\sigma_{11}-\sigma_{22})^2 + 2(\sigma_{23})^2 + 2(\sigma_{13})^2 + 2(\sigma_{12})^2, \quad (1)$$

where $\overline{\sigma}$ is the equivalent stress and σ_{11}, σ_{22}, σ_{33}, σ_{23}, σ_{13} and σ_{12} are the components of the Cauchy stress tensor. The hardening behaviour is described by the Voce law [30, 31]

$$Y = Y_0 + (Y_{sat}-Y_0)\left\{1-\exp\left(-C_y\left(\overline{\varepsilon}^{\,p}\right)\right)\right\}, \quad (2)$$

since aluminium alloys are prone to exhibit saturation of the hardening behaviour. In Eq. (2), $\overline{\varepsilon}^{\,p}$ denotes the equivalent plastic strain, Y_0 is the initial value of the flow stress, Y_{sat} is the flow stress saturation value and C_y defines the growth rate of the yield surface. These parameters were identified based on tensile test results [16] and their values are presented in Table 2. Besides, the elastic behaviour is assumed isotropic and constant, which is described by the Hooke's law using the

Table 2 Elastic properties and Voce hardening law parameters of the 6016-T4 aluminium alloy [16]

Elastic Properties		Voce Law		
Young's modulus (GPa)	Poisson's ratio	Y_0 [MPa]	Y_{sat} [MPa]	C_y
69	0.30	131.4	312.3	12.08

parameters also listed in Table 2.

The friction between the blank and the forming tools is modelled through the classical isotropic Coulomb's law. The value of the friction coefficient used in the numerical simulations is $\mu = 0.15$ and was adjusted in order to minimize the difference between the experimental and numerical punch force evolution during the drawing stage [16].

Stress analysis procedure

Springback defines the geometrical change of a part after forming, when the forces imposed by the forming tools are removed. The accuracy of the springback prediction is strongly dictated by the stress state obtained after forming, particularly the gradient through the sheet thickness. Most of the studies on the analysis of residual stress and springback, induced by the forming process, are based on simple bending [9, 11, 24] and straight flanging [32]. For instance, the analysis of plane strain bending tests was fundamental to understand the role of a superimposed tension force in the sensitivity of springback prediction to numerical parameters, such as the number of through thickness integration points and the integration rule [12, 24].

A cylindrical cup is an axisymmetric component, as well as the ring cut from its wall. At the end of the forming process, the cup's vertical wall is submitted to residual stresses, which are usually evaluated using the cylindrical coordinate system schematically shown in Fig. 3. The cut of the ring from the cup's vertical wall contributes to the release of the radial (σ_{rr}) and axial (σ_{zz}) residual stresses. When the ring is split, the two ends of the ring open a distance that is proportional to the circumferential residual stress ($\sigma_{\theta\theta}$) [2, 3, 7, 8]. In fact, based on this knowledge, a methodology was proposed to estimate the residual stresses using the gap opening, assuming that the circumferential residual stress presents an axisymmetric distribution and it does not change along the height of ring. This methodology is based on the assumption that the elastic closing of the ring can be simplified as pure bending of a curved beam, enabling the definition of an applied bending moment, equivalent to the one generated by the ring opening [2].

This axial moment per unit length results from the through-thickness distribution of the circumferential stresses and can be evaluated as

$$M_z = \int_{-t/2}^{t/2} \sigma_{\theta\theta} \eta d\eta, \tag{3}$$

where η is the through-thickness local coordinate and t is the final sheet thickness. This enables its evaluation for each section, along the height of ring or along the circumferential direction. In this study, this moment is evaluated using the six through-thickness integration points, as schematically shown in Fig. 3, which are labelled according to their relative position. The Gauss Point (GP) located closest to the surface in contact with the punch (inner surface) is GP1 and the one closest to the surface in contact with the die (outer surface) is GP6. Also, according to the through-thickness coordinate η definition, GP1 presents always the lowest (negative) coordinate while GP6 presents always the highest (positive) coordinate. The numerical evaluation of this moment is performed using the Gauss integration rule, assuming two integration points for each finite element, such that

$$M_z = \frac{t}{6} \sum_{i=1}^{6} \sigma_{\theta\theta}(\eta_i)\eta_i. \tag{4}$$

The analysis of the through-thickness stress distributions and the axial moment will be always performed for the sections located closer to the split plane. This sections are representative of all sections situated along the circumferential direction, at the same cup height, since the isotropic von Mises yield criterion is adopted.

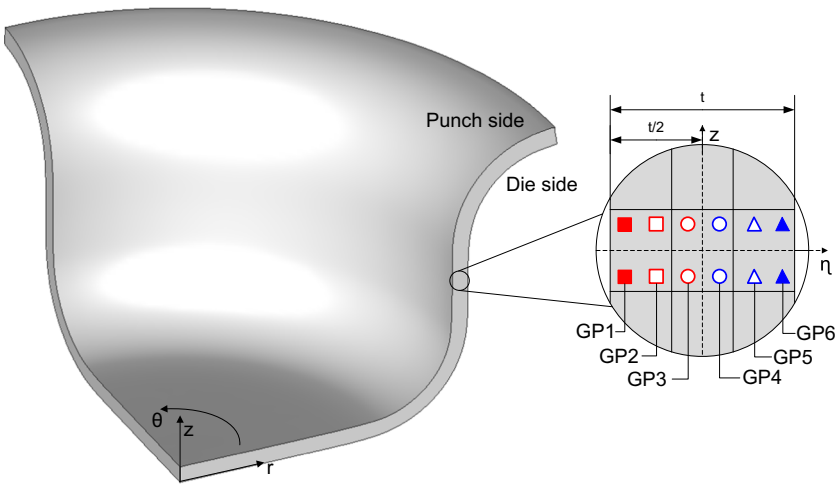

Fig. 3 Positioning of the cylindrical coordinate system in the formed cup and the local coordinate system η for the through-thickness stress analysis

Results and discussion

The numerical simulation of the deep drawing of the cylindrical cup was performed, considering the two different values of gap between the die and the punch. Figure 4 presents the punch force evolution with its displacement, highlighting the difference in the initial evolution but also on the final stage. In fact, for both cases the maximum punch force is attained for a displacement that corresponds to the instant that the die and the punch shoulder radii are completely formed in the part. However, while for the gap of 1.125 mm (labelled "Lower gap") this occurs for a punch displacement of 11–12 mm, for the gap of 4 mm (labelled "Higher gap"), this occurs only for approximately 16 mm. Moreover, for the lower gap condition the ironing stage starts to occur for a punch displacement of approximately 21 mm, while for the other condition no ironing occurs. For the lower gap condition, the maximum thickness value measured in the cup's flange, for a punch displacement of 20 mm (i.e. before the ironing stage), was approximately 1.3 mm. Therefore, the theoretical thickness reduction induced by the ironing stage is 15% [33], which can be considered a small value. The geometry of both cups is also quite different, as shown in Fig. 5, including their height. This results from the fact that different gap values induce a different thickness distribution along the cup wall, as shown in Fig. 6. In particular, a stronger thickness reduction is observed for the higher gap in the region in contact with the punch radius.

For the lower gap value, higher thinning occurs at the entrance to the punch radius section and the confluence of the punch radius with the cup wall, as previously reported in [16]. For the higher gap value, higher thinning also occurs at the entrance to the punch radius section, but a value similar to the initial one is observed afterwards, followed by a thickening with a slope similar to the one observed for the lower gap value (see Fig. 6). Moreover, for the higher gap value the cup's bottom also presents higher thinning values, which leads to a higher cup, for the same drawing depth. This effect can also be

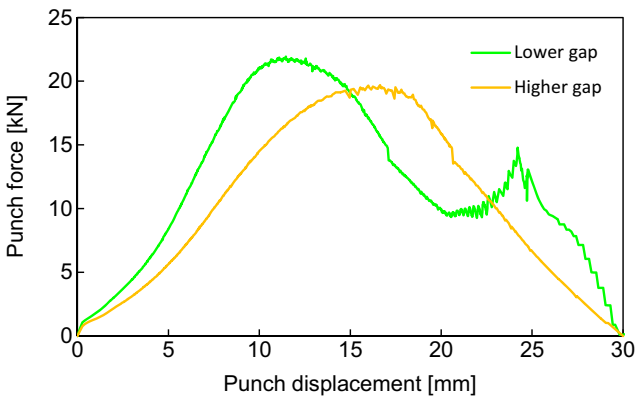

Fig. 4 Numerical punch force evolution for the two different values of gap between the die and the punch

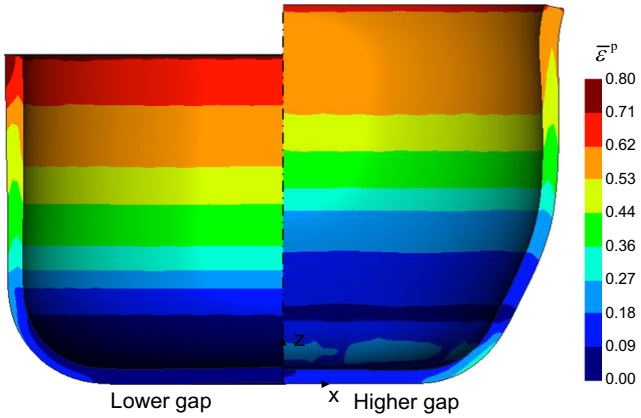

Fig. 5 Equivalent plastic strain distribution plotted on the final shape of the cylindrical cups

observed in the equivalent plastic strain distribution shown in Fig. 5. Although not shown here, the strong thinning observed for the higher gap value can be reduced by decreasing either the friction coefficient or the blank-holder force, but the trend remains unaltered. Thus, the trend for the thickness distribution is mainly dictated by the clearance between the punch and the die.

Finally, it should be mentioned that since there is no blank-holder stopper (see Fig. 1), the blank-holder only stops its vertical movement when it establishes contact with the die. Therefore, there is always some squeezing of the edge of the cup, resulting from the contact with the blank-holder [28, 29, 34].

Three rings were cut from each of the cups (see Fig. 2 (a)) and split, in order to evaluate the opening. The results are presented in Table 3, highlighting that for the lower gap value there is a clear trend for the decrease of the opening with the increase of the distance from the cup's bottom, as observed experimentally. Globally, the experimental results are accurately predicted, except for the top ring, for which the ring opening is clearly overestimated. This is certainly related with

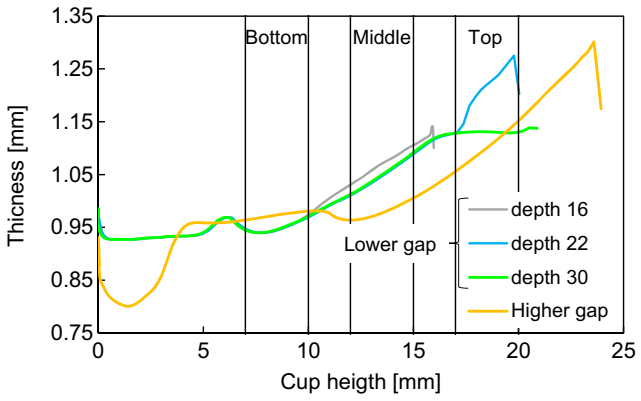

Fig. 6 Thickness distribution along the cup height at the end of the cup forming and unloading stage, for the standard punch displacement of 30 mm, for both gap values, and for the punch displacement of 16 and 22 mm for the lower gap value

Table 3 Numerical ring opening values at different positions and considering distinct process conditions. The values presented between brackets for the lower gap, full drawn cup, correspond to the experimental ones

	Punch displacement [mm]			
	30 (Full drawn cup)		16	22
Ring	Lower gap	Higher gap	Lower gap	
Bottom	6.37 (5.67)	3.59*	7.30	5.98
Middle	4.08 (4.23)	6.94	-	-
Top	3.20 (2.12)	4.05	-	-

* This ring presents an accentuated curvature in the axial direction

the underestimation of the thickening predicted by the von Mises yield criterion, for the material located under the blank-holder [29].

For the higher gap, the middle ring presents the higher opening value. This trend is similar to the one reported in [3], in the analysis of a 6111-T4 aluminium alloy, considering a similar gap with different tools dimensions. Nonetheless, it should be mentioned that for the higher gap value the bottom ring presents an accentuated curvature in the axial direction, as highlighted in the sections profiles shown in Fig. 7. A more pronounced conical shape of the ring is known to lead to a slight decrease of the ring opening [4]. Moreover, Fig. 7 also presents the relative position of the lines corresponding to the six integration points. The axial moment resulting from the residual circumferential stresses is evaluated based on the Gauss points of each element for a specific range of the longitudinal axis z, which depends on the value of the gap between the die and the punch. When the cup wall is not vertical, the Gauss points of the stacked finite elements are not aligned with the radial direction, as highlighted in Fig. 7. Therefore, the bottom ring obtained for the higher gap value will be discarded in the following analysis of the axial moment distribution along the cup wall.

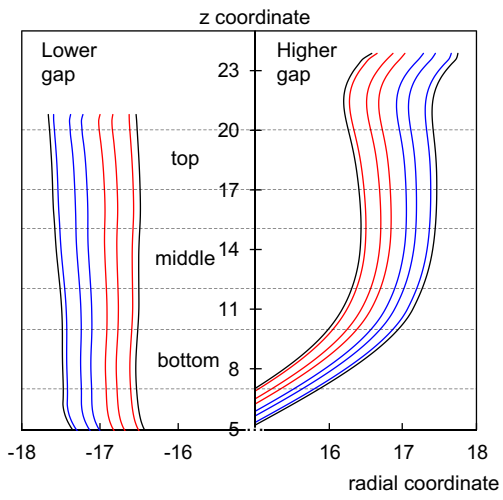

Fig. 7 Section profile of the cup wall at the end of the forming and unloading stages, highlighting the relative position of the six through-thickness integration points (red lines for the points located closer to the punch and blue lines for the ones closer to the die, as in Fig. 3)

Stress distributions

In this section the stress distributions along the cup wall are analysed, first for the cups formed to a drawing depth of 30 mm and afterwards for the two other values considered.

Analysis of the three rings

Figure 8 presents the axial stress distribution along the cups wall at the end of the forming and unloading stage, for both conditions under analysis. The through-thickness gradient is closely related with the fact that the material was bent over the die radius and straightened at the exit of the die edge, presenting a compressive value in the inner surface and a tensile one in the outer surface. The same trend is observed for the circumferential stress distribution, as shown in Fig. 9, which is in agreement with the results previously reported in [13]. Moreover, the ironing stage contributes to a change on the

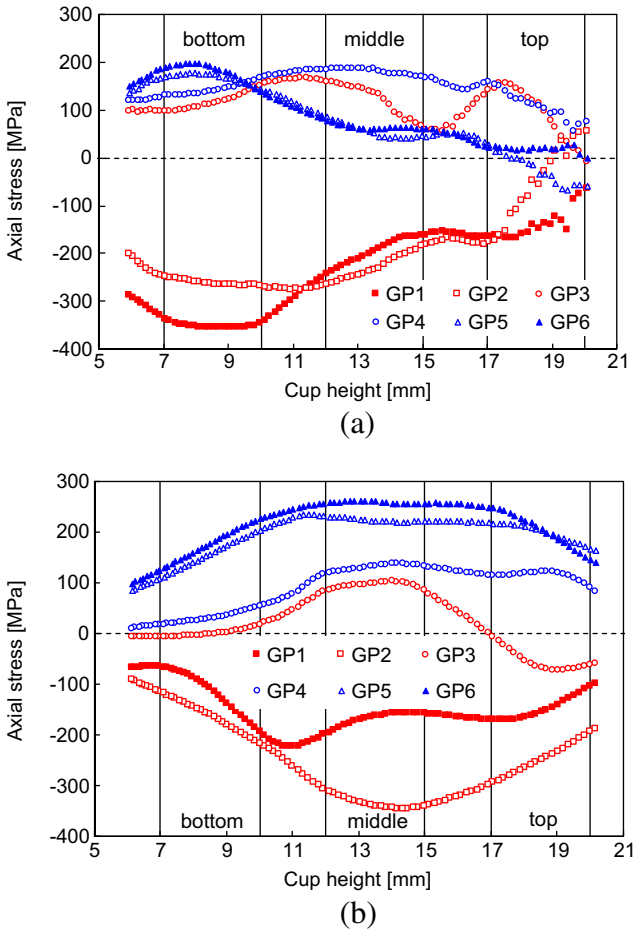

Fig. 8 Axial stress distributions along the cup wall at the end of the cup forming and unloading stage: (**a**) Lower gap; (**b**) Higher gap

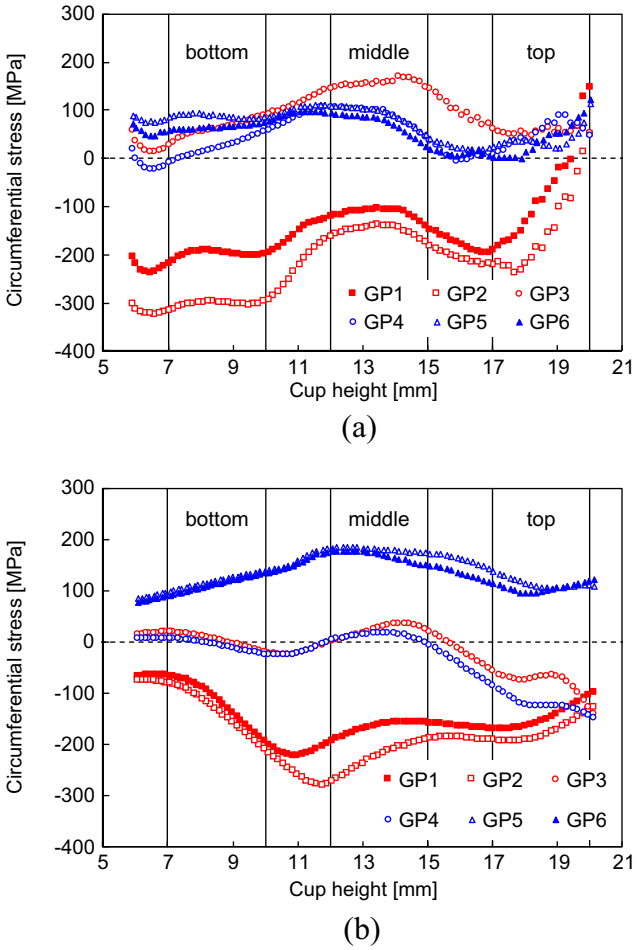

Fig. 9 Circumferential stress distributions along the cup wall at the end of the cup forming and unloading stage: (**a**) Lower gap; (**b**) Higher gap

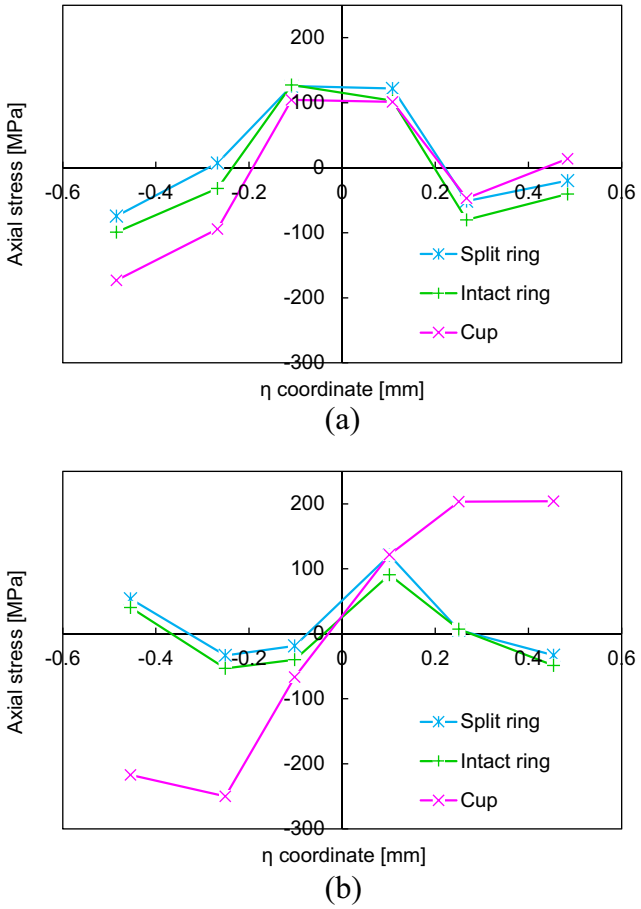

Fig. 10 Axial stress distributions along the middle section of the Top ring at the end of the forming and unloading stage, in the intact ring and in the split-ring: (**a**) Lower gap; (**b**) Higher gap

profile of both components, in particular to a reduction of the tensile residual stress values in the outer surface [13]. The radial stress distribution is not shown, since it presents a negligible magnitude when compared with the other stress components.

Figure 10 presents the through-thickness axial stress distribution in the middle section of the top ring ($z = 18.5$ mm), both for the cup, the intact ring and the split-ring. The trimming of the ring from the cup clearly contributes to the release of the axial residual stress component, while the split only has a small impact in the stress distribution, as expected. Moreover, the reduction of this stress component with the cut of the ring from the cup wall is more evident for the higher gap value. In fact, the axial stress distribution at the end of the forming process presents a distribution typical of a bending process and an "S"-curve shape after the trimming, which is typical of the unloaded state [7]. The release of the axial stress component is accompanied by the reduction of the circumferential stress component, as shown in Fig. 11. These figures highlight the interdependency between these two stress components during the ring cut stage, where the lower gap also presents a smaller variation of the circumferential stress component. The intact ring presents a through-thickness circumferential stress distribution analogous to that of a plastically bent beam in a loaded configuration, which is responsible for generating the ring opening. The stress trend observed for the intact ring obtained with the higher gap is more similar to the one previously reported in [7], although in the example under analysis the neutral line is clearly shifted to the outer surface (see Fig. 11 (b)). Besides, the neutral line location is identical to the one observed in the cup. The analysis of the circumferential stress distribution along the cup wall presented in Fig. 9, shows that there is a change of the neutral line location in function of the position along the vertical wall. For instance, for the lower gap value it is clearly shifted to the inner surface for material points located in the bottom and middle ring. In fact, the change of the circumferential stresses with the axial position has been pointed out in the literature [13, 35], with some authors reporting an increase from the mid-line towards the cup bottom [7]. Taking as reference the results shown in Fig. 9 for the cup, this trend will certainly depend on the forming parameters. Consequently, the results correlate well

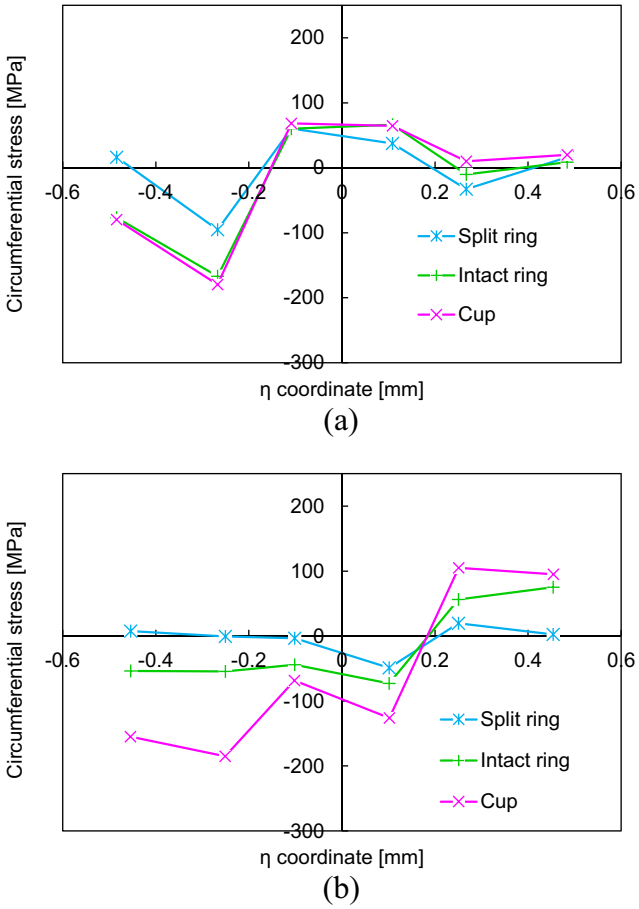

Fig. 11 Circumferential stress distributions along the middle section of the Top ring at the end of the forming and unloading stage, in the intact ring and in the split-ring: (**a**) Lower gap; (**b**) Higher gap

with the fact that the ring opening is sensitive to the vertical position along the cup wall [4] or even to the ring height [1].

The ring split stage induces a significant change in the circumferential stress distribution, which now also exhibits the "S"-curve shape, typical of the plastically bent beam in an unloaded configuration [7]. The results indicate that the axial moment for the middle section of the ring is not necessarily null, but its integration along the ring height leads to a zero value. In order to better understand the effect of the split stage, Fig. 12 presents the circumferential stress distributions obtained for the intact and split middle ring, for both gap values. This ring was selected because it presents, globally, the higher values for the ring opening and the trend observed is similar for all rings. The effect of the split is evident in the reduction of the stress values in the ring, which still presents residual stresses. The through-thickness circumferential residual stress presents an almost axisymmetric distribution, with exception of the sections located closer to the split plane, where the minimum values are attained. Moreover, there is also a gradient in the circumferential residual stresses along the ring height. It should be mentioned that, for the lower gap value, the stress distribution in the intact ring is not as axisymmetric as for the higher gap due to the fact that the ironing stage is more sensible to small shape errors induced by the tool description with Nagata patches [36].

Figure 13 presents the circumferential stress change induced by the split of the top ring, determined as the difference between the intact and the split-ring (see Fig. 11). The results obtained for the higher gap value present a more linear trend for the stress change, identical to the one previously reported in [8], while for the lower gap value the linear tendency is not so clear, although both top rings present no inelastic effects.

Analysis of the bottom ring

For the lower gap value, the analysis of the bottom ring was also performed for two other values of punch displacement, namely 16 mm and 22 mm. For a punch displacement of 16 mm the blank is still in contact with the blank-holder, presenting a small flange. The positioning of the ring is schematically shown in Fig. 2 (b). For the punch displacement of 22 mm the ironing stage has already started, but with a small value of thickness reduction (see Fig. 4 and Fig. 6). Figure 14 (a) presents the circumferential stress distribution along the middle section of the bottom ring, before the ring was cut from the cup wall, for 16 mm, 22 mm and 30 mm of punch displacement. Figure 14 (b) shows the same results obtained for the intact rings. It should be mentioned that the bottom ring is located in a region not submitted to ironing. However, as shown in Fig. 6, the ironing stage induces increased stretching, i.e. the true strains in the cup bottom become higher, acting as a stress relief and reducing the stress magnitudes [8]. In fact, as previously reported in [4], as the cup is drawn deeper, the fraction of uniform plastic strain in the cup wall increases. As a result, the material in the cup wall is deformed significantly past the yield stress, and the magnitude of the through-thickness strain inhomogeneities (difference in plastic strain from one location to another) introduced by the bending and unbending of the blank decreases. Moreover, in terms of the stress-strain curve of the material, the deformation of the entire cup wall proceeds into the strain region where large strain differences correspond to relatively small stress differences, particularly if the material hardening behaviour is well described by a saturation law.

Smaller stress differences translates into reduced residual stresses and springback. This interpretation of the influence of the drawing depth presented in [4], is corroborated by the equivalent plastic strain distribution along the cup wall, shown in Fig. 15 for the drawing depth of 16, 22 and 30 mm. In this figure it also visible the influence of the ironing stage, particularly for the outer surface, for which a higher increase is observed when compared with the inner surface, which correlates with the strong reduction of the axial component of the residual stress. Thus, as shown in Table 3, the bottom ring cut from the cup obtained with only 16 mm of punch

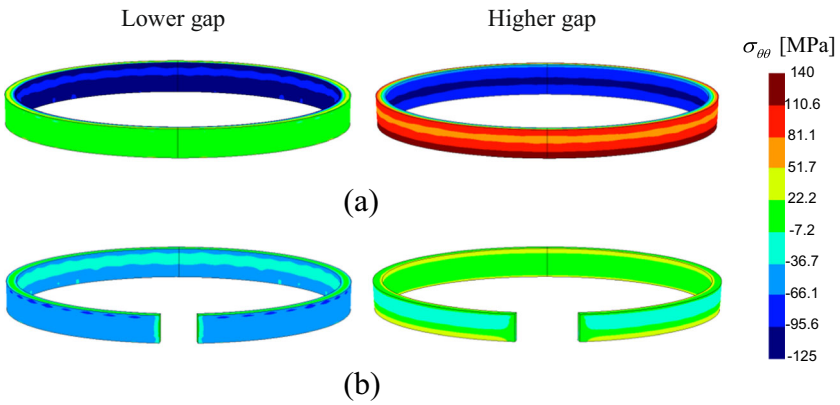

Fig. 12 Circumferential stress distributions in the Middle ring: (**a**) intact and (**b**) after the split

displacement is the one presenting the higher ring opening. However, as shown in Fig. 14 (a), the increase of the plastic strain does not necessary means the decrease of the magnitude of the through-thickness stress inhomogeneities, since similar equivalent stress values can be obtained for different stress states. Thus, the bottom ring cut from the fully drawn cup (depth 30 mm) presents a higher ring opening than the one obtained from a cup obtained with a punch displacement of 22 mm. These results show that the circumferential stress through-thickness distribution is clearly modified by the ironing stage, even for physical locations in the cup wall positioned far away from the material that is submitted to this compression state. In fact, for the full drawn cup, the trend of the circumferential stress through-thickness distribution obtained for the bottom ring is similar to the one obtained for the top ring (see Fig. 11 (a)). However, as previously stated, the ironing stage contributes to a more uniform magnitude of the circumferential stress along the thickness, which leads to a smaller ring opening.

Axial moment distributions

The axial moment per unit length, evaluated along the cup and in the ring wall, using Eq. (4), is presented in Fig. 16, for the

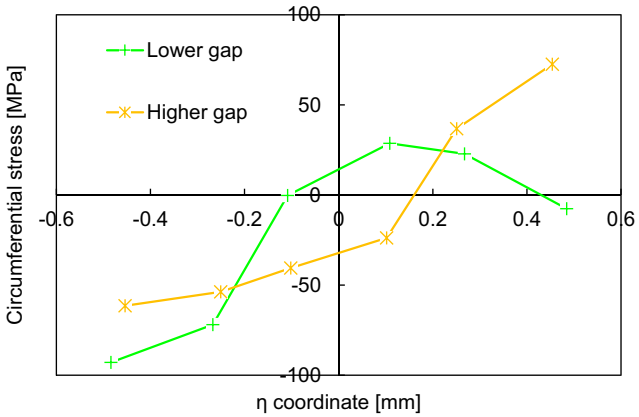

Fig. 13 Difference between the circumferential stress distributions in the intact ring and in the split-ring, at the middle section of the Top ring

through-thickness section located closer to the split position. The comparison between the values determined for the cup wall and the intact ring confirm the release of the circumferential stresses induced by the cut of the ring from the cup's wall. Moreover, the influence of the ironing stage that occurs for the lower gap, mainly for the last 5 mm of the cup's wall (see Fig. 6), is quite notorious in the smaller difference between the axial moments observed for the top ring, when

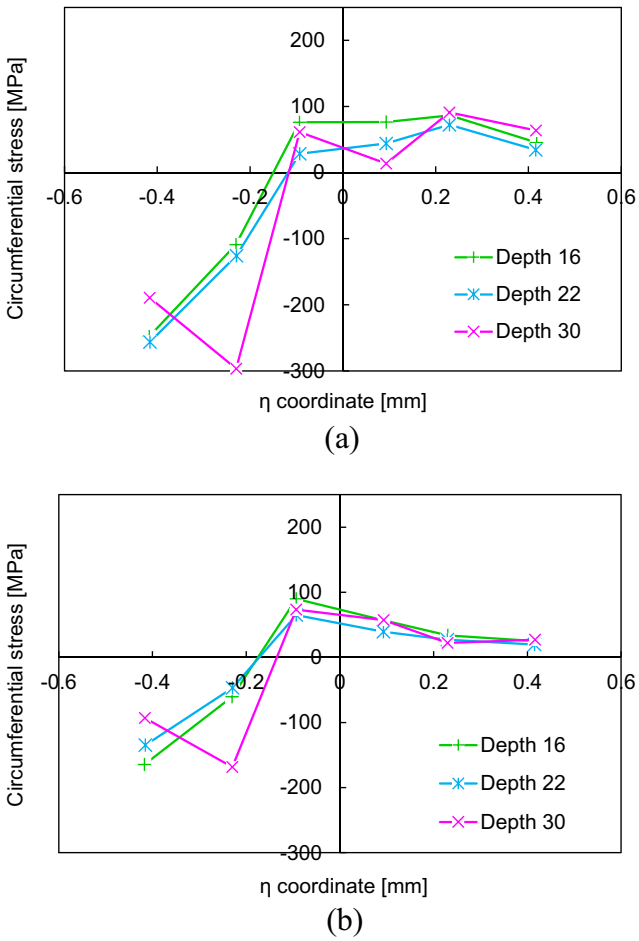

Fig. 14 Circumferential stress distributions along the middle section of the Bottom ring, obtained with the Lower gap: (**a**) at the end of the cup forming and unloading stage, (**b**) in the intact ring

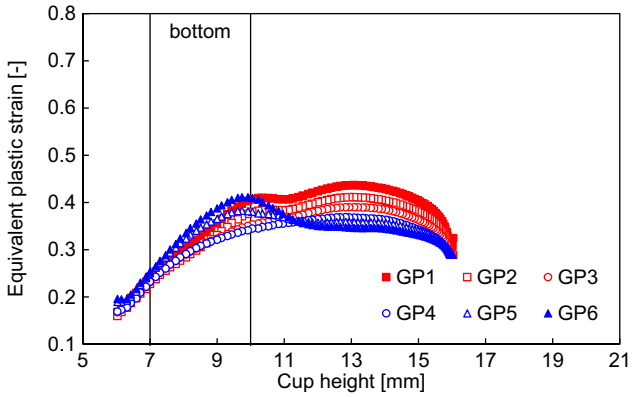

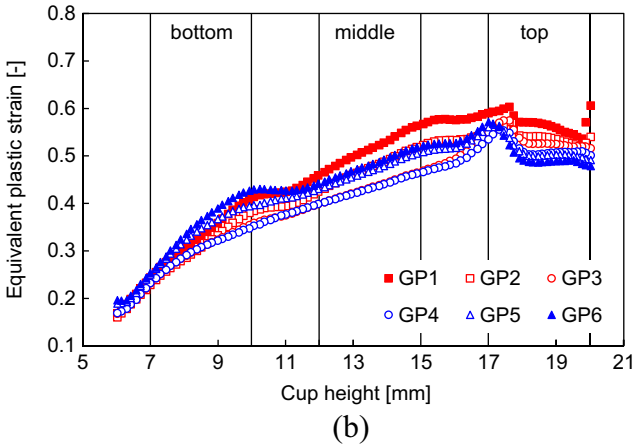

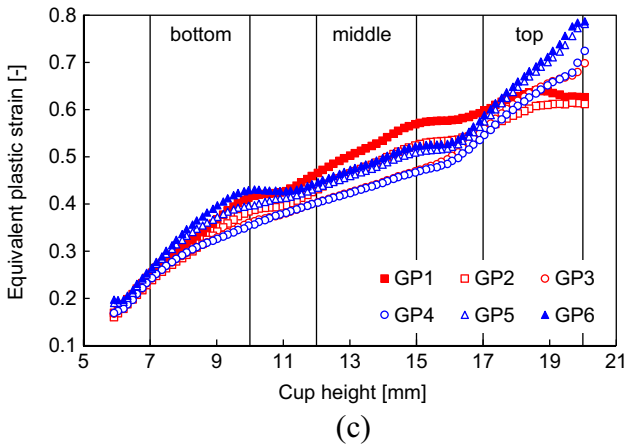

Fig. 15 Equivalent plastic strain distributions along the cup wall at the end of the cup forming and unloading stage, considering the lower gap value, for a punch displacement of: (**a**) 16 mm; (**b**) 22 mm and (**c**) 30 mm (full drawn)

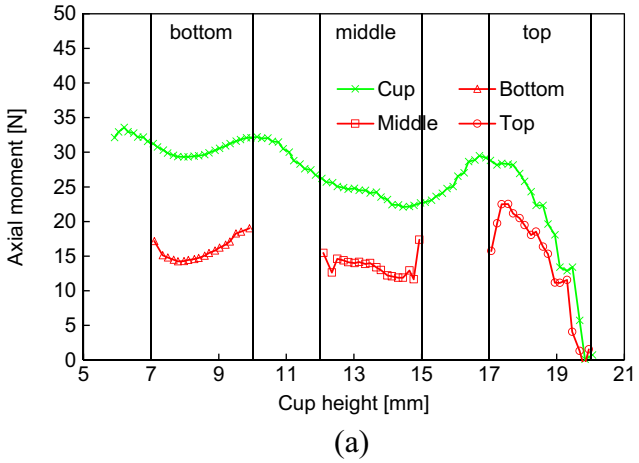

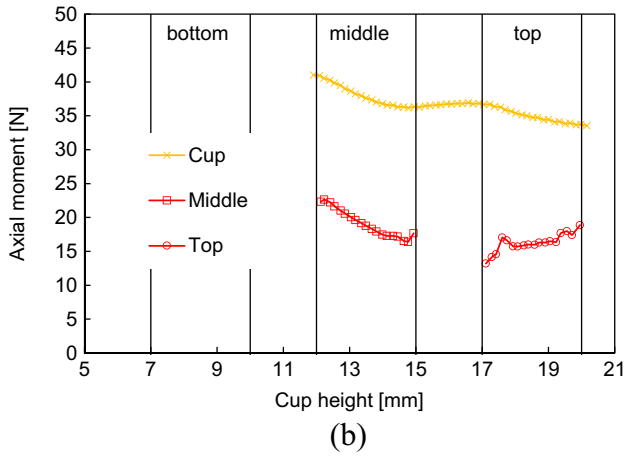

Fig. 16 Axial moment (per unit length) distributions along the cup wall at the end of the cup forming and unloading stage and in the intact ring for: (**a**) Lower gap; (**b**) Higher gap

compared with the other rings (see Fig. 16 (a)). This seems to result from the more uniform through-thickness distributions predicted in the cup for both the axial and the circumferential stresses (see Fig. 8 and Fig. 9). As discussed before for the top ring, the ironing operation changes the axial stress distribution, affecting the residual stresses predicted for the intact ring. The results confirm that the ironing changes the stress distribution, with a clear impact on the residual stresses in the cup and in the intact ring. The change in the residual stresses depends of the thickness reduction induced by the ironing operation [13], but its effect is evident even for small values as the one tested in this work.

Globally, the axial moments predicted for the higher gap condition are always higher than the ones obtained for the lower gap, which correlates with the through-thickness circumferential stress distributions along the cup wall (see Fig. 9) and with the ring opening values predicted for the middle and top rings (see Table 3). It is interesting to note that for the material located in the top ring the axial moment changes its trend upon the release of the axial stresses, which can be related with its evolution in the cup (see Fig. 8). All other axial moments present a similar trend when evaluated for the cup or the intact ring.

For both gap values, the average axial moment decreases with the increase of the distance from the cup bottom, which is in agreement with the trend observed for the opening of the rings. Moreover, in both cases it is possible to observe that the axial moment is not

constant along the cup wall, which correlates well with the sensitive of the ring opening to the positioning along the cup wall [1, 4]. In fact, even when no ironing occurs, the axial moment varies along the ring height (see Fig. 16 (b)). Nevertheless, for a higher gap value it is clear that the axial moment presents a smaller variation, which can be related with the smaller variation of the axial stress along the axial direction (see Fig. 8 (b)), associated to a smaller stretch effect (see Fig. 6) [7]. This shows that the stretch effect can also be related with the clearance between the die and the punch, besides the blank-holder force.

Figure 17 presents the axial moment distributions along the cup and the intact ring height, obtained for 16, 22 and 30 mm of punch displacement. The axial moment distributions are quite similar at the end of the cup forming and unloading, which is coherent with the fact that this part of the cup already attained a stable shape for a punch displacement of 16 mm (see also Fig. 6). Nevertheless, as shown in Fig. 14 (a), the through-thickness stress distributions are different, which confirms that similar axial moments can be determined for different stress distributions. Regarding the axial moment distribution in the intact ring, the trend is quite similar for the three depths, presenting an average value that is coherent with the ring opening values presented in Table 3, i.e. the one obtained with a drawing depth of 16 mm presents the higher value, followed by the one obtained from the full drawn cup and, finally, the one extracted from the cup obtained with a drawing depth of 22 mm. The increase in the relative difference for the axial moment evaluated in the intact ring for the three punch depths is related with the different distribution of the axial component of the residual stress, since the release of this component contributes to the change circumferential stress distribution (see Fig. 14), as discussed in the previous section.

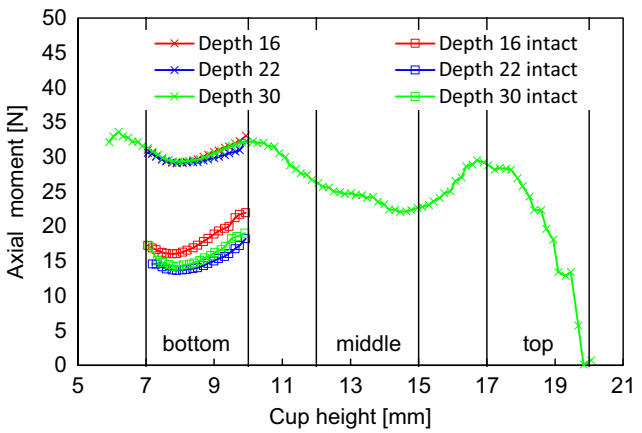

Fig. 17 Axial moment (per unit length) distributions along the cup wall at the end of the cup forming and unloading stage and in the intact ring for the Lower gap, using different punch displacements

Conclusions

The results show that deep drawn cups present axial and circumferential residual stresses of high magnitude, which are tensile at the outer surface and compressive at the inner surface, with profiles similar to what is expected from a bending-unbending operation [8, 13]. The ironing of the vertical wall changes the stress distribution along the cup wall outer surface, with a decrease of the axial stresses from a maximum near to the cup bottom to a minimum along the wall, while the circumferential residual stresses are distributed more uniformly along the cup wall [13]. This change in the characteristic residual stresses distribution is observed in all cup wall, i.e. it is not limited to the material that was submitted to the through-thickness compression state. Moreover, as stated in [13], the reduction in the residual stresses after deep drawing and ironing is observed even for relatively small ironing strains.

The axial and circumferential stress profiles exhibit a strong dependence on the axial position, which reflects the effect of bending under stretching. This effect is dictated by the blank-holder force selected, but also by the clearance between the die and the punch. The cut of the ring from the cup releases the residual axial stress component, as well as a part of the circumferential stress component, presenting an interdependency between these two components. In fact, since the ironing stage induces a more uniform through-thickness distribution of the axial stress component in the cup, the variation of the circumferential stresses between the cup and the intact ring is also smaller. Globally, the introduction of an ironing stage contributes to the reduction of the circumferential stress component through-thickness gradient, leading to a smaller ring opening, as observed also in [2]. However, this effect depends on the vertical position of the ring and the drawing depth, since the ironing stage changes the characteristic distribution of the residual stress component. The trend observed for several rings cut along the cup wall reflect the strong dependence on the axial position of both the axial and circumferential through-thickness residual stress profiles, which are strongly affected by a relatively small ironing strain.

Acknowledgements The authors gratefully acknowledge the financial support of the Brittany Region (France), the Portuguese Foundation for Science and Technology (FCT), under projects PTDC/EMS-TEC/0702/2014 (POCI-01-0145-FEDER-016779) and PTDC/EMS-TEC/6400/2014 (POCI-01-0145-FEDER-016876), and by UE/FEDER through the program COMPETE 2020. The first and the third author are also grateful to the FCT for the Doctoral grant SFRH/BD/90669/2012 and the Postdoctoral grant SFRH/BPD/101334/2014, respectively.

Compliance with ethical standards

Conflict of interest None.

References

1. Demeri MY, Lou M, Saran MJ (2000) A benchmark test for springback simulation in sheet metal forming. doi:10.4271/2000-01-2657
2. Xiao L-H, Yuan D-H, Xiang J-Z et al (2016) Residual stress in the cylindrical drawing cup of SUS304 stainless steel evaluated by split-ring test. Acta Mech Sinica 32:125–134. doi:10.1007/s10409-015-0516-4
3. Xia ZC, Miller CE, Ren F (2004) Springback behavior of AA6111-T4 with split-ring test. In: AIP Conf. Proc., pp 934–939. doi:10.1063/1.1766647
4. Foecke T, Gnaeupel-Herold T (2006) Robustness of the sheet metal springback cup test. Metall Mater Trans A 37:3503–3510. doi:10.1007/s11661-006-1045-3
5. Laurent H, Grèze R, Manach PY, Thuillier S (2009) Influence of constitutive model in springback prediction using the split-ring test. Int J Mech Sci 51:233–245. doi:10.1016/j.ijmecsci.2008.12.010
6. Laurent H, Greze R, Oliveira MC et al (2010) Numerical study of springback using the split-ring test for an AA5754 aluminum alloy. Finite Elem Anal Des 46:751–759. doi:10.1016/j.finel.2010.04.004
7. Gnaeupel-Herold T, Prask HJ, Fields RJ et al (2004) A synchrotron study of residual stresses in a Al6022 deep drawn cup. Mater Sci Eng A 366:104–113. doi:10.1016/j.msea.2003.08.059
8. Gnaeupel-Herold T, Foecke T, Prask HJ, Fields RJ (2005) An investigation of springback stresses in AISI-1010 deep drawn cups. Mater Sci Eng A 399:26–32. doi:10.1016/j.msea.2005.02.017
9. Oliveira MC, Alves JL, Chaparro BM, Menezes LF (2007) Study on the influence of work-hardening modeling in springback prediction. Int J Plast 23:516-543. doi: 10.1016/j.ijplas.2006.07.003
10. Lee MG, Kim SJ, Wagoner RH et al (2009) Constitutive modeling for anisotropic/asymmetric hardening behavior of magnesium alloy sheets: application to sheet springback. Int J Plast 25:70–104. doi:10.1016/j.ijplas.2007.12.003
11. Li KP, Carden WP, Wagoner RH (2002) Simulation of springback. Int J Mech Sci 44:103–122. doi:10.1016/S0020-7403(01)00083-2
12. Meinders T, Burchitz IA, Bonte MHA, Lingbeek RA (2008) Numerical product design: Springback prediction, compensation and optimization. Int J Mach Tools Manuf 48:499–514. doi:10.1016/j.ijmachtools.2007.08.006
13. Ragab MS, Orban HZ (2000) Effect of ironing on the residual stresses in deep drawn cups. J Mater Process Technol 99:54–61. doi:10.1016/S0924-0136(99)00360-X
14. Laurent H, Coër J, Manach PY et al (2015) Experimental and numerical studies on the warm deep drawing of an al-mg alloy. Int J Mech Sci 93:59–72. doi:10.1016/j.ijmecsci.2015.01.009
15. Manach P-Y, Coër J, Laurent AJH et al (2016) Benchmark 3 - Springback of an al-mg alloy in warm forming conditions. J Phys Conf Ser 734:22003. doi:10.1088/1742-6596/734/2/022003
16. Simões VM, Laurent H, Oliveira MC, Menezes LF (2016) Natural aging effect on the forming behavior of a cylindrical cup with an al-mg-Si alloy. In: AIP Conf. Proc, p 200021:1–6. doi:10.1063/1.4963639
17. Menezes LF, Teodosiu C (2000) Three-dimensional numerical simulation of the deep-drawing process using solid finite elements. J Mater Process Technol 97:100–106. doi:10.1016/S0924-0136(99)00345-3
18. Oliveira MC, Alves JL, Menezes LF (2008) Algorithms and strategies for treatment of large deformation frictional contact in the numerical simulation of deep drawing process. Arch Comput Methods Eng 15:113-162. doi:10.1007/s11831-008-9018-x
19. Menezes LF, Neto DM, Oliveira MC, Alves JL (2011) Improving computational performance through HPC techniques: case study using DD3IMP in-house code. AIP Conf Proc. 1353: 1220-1225. doi:10.1063/1.3589683
20. Neto DM, Oliveira MC, Menezes LF (2015) Surface smoothing procedures in computational contact mechanics. Arch Comput Methods Eng 24:37–87. doi:10.1007/s11831-015-9159-7
21. Barros PD, Baptista AJ, Alves JL et al (2015) Trimming of 3D solid finite element meshes: sheet metal forming tests and applications. Eng Comput 31:237–257. doi:10.1007/s00366-013-0344-8
22. Baptista AJ, Alves JL, Rodrigues DM, Menezes LF (2006) Trimming of 3D solid finite element meshes using parametric surfaces: application to sheet metal forming. Finite Elem Anal Des 42: 1053–1060. doi:10.1016/j.finel.2006.03.005
23. Hughes TJR (1980) Generalization of selective integration procedures to anisotropic and nonlinear media. Int J Numer Methods Eng 15:1413–1418. doi:10.1002/nme.1620150914
24. Wagoner RH, Li M (2007) Simulation of springback: through-thickness integration. Int J Plast 23:345–360. doi:10.1016/j.ijplas.2006.04.005
25. Neto DM, Oliveira MC, Menezes LF, Alves JL (2014) Applying Nagata patches to smooth discretized surfaces used in 3D frictional contact problems. Comput Methods Appl Mech Eng 271:296-320. doi: 10.1016/j.cma.2013.12.008
26. Neto DM, Oliveira MC, Menezes LF, Alves JL (2013) Nagata patch interpolation using surface normal vectors evaluated from the IGES file. Finite Elem Anal Des 72: 35-46. doi:10.1016/j.finel.2013.03.004
27. Nagata T (2005) Simple local interpolation of surfaces using normal vectors. Comput Aided Geom Des 22:327–347. doi:10.1016/j.cagd.2005.01.004
28. Neto DM, Martins JM, Cunha PM et al Thermo-mechanical finite element analysis of the AA5086 alloy under warm forming conditions. Submitted to Int J Solids Struct. http://hdl.handle.net/10316/40114. Accessed 30 March 2017
29. Coër J, Laurent H, Oliveira MC et al Detailed experimental and numerical analysis of a cylindrical cup deep drawing. Submitted to Int J Mater Form. http://hdl.handle.net/10316/40113. Accessed 30 March 2017
30. Voce E (1948) The relationship between stress and strain for homogeneous deformations. J Inst Met 74:537–562
31. Voce E (1955) A practical strain-hardening function. Meta 51:219–226
32. Livatyali H, Altan T (2001) Prediction and elimination of springback in straight flanging using computer aided design methods: part 1. Experimental investigations J Mater Process Technol 117:262–268. doi:10.1016/S0924-0136(01)01164-5
33. Danckert J (2001) Ironing of thin walled cans. CIRP Ann - Manuf Technol 50:165–168. doi:10.1016/S0007-8506(07)62096-4
34. Rabahallah M, Bouvier S, Balan T, Bacroix B (2009) Numerical simulation of sheet metal forming using anisotropic strain-rate potentials. Mater Sci Eng A 517:261–275. doi:10.1016/j.msea.2009.03.078
35. Yuying Y, Chunfeng L, Hongzhi X (1992) A study of longitudinal cracking and the forming technology for deep-drawn austenitic stainless-steel cups. J Mater Process Technol 30:167–172. doi:10.1016/0924-0136(92)90344-R
36. Neto DM, Oliveira MC, Alves JL, Menezes LF (2014) Comparing faceted and smoothed tool surface descriptions in sheet metal forming simulation. Int J Mater Form 8:549–565. doi:10.1007/s12289-014-1177-8